Mitochondrial respiration and genomic analysis provide insight into the influence of the symbiotic bacterium on host trypanosomatid oxygen consumption.

Allan C. Azevedo-Martins, A. C. L. Machado, Cecilia Coimbra Klein, L. Ciapina, Luiz Gonzaga, Ana Tereza Ribeiro Vasconcelos, Marie-France Sagot, Wanderley De Souza, Marcelo Einicker-Lamas, Antonio Galina, et al.

Mitochondrial respiration and genomic analysis provide insight into the influence of the symbiotic bacterium on host trypanosomatid oxygen consumption

A. C. AZEVEDO-MARTINS[1,2], A. C. L. MACHADO[1,2], C. C. KLEIN[3,4], L. CIAPINA[5], L. GONZAGA[5], A. T. R. VASCONCELOS[5], M. F. SAGOT[3,4], W. DE SOUZA[1,2,6], M. EINICKER-LAMAS[7], A. GALINA[8]* *and* M. C. M. MOTTA[1,2]*

[1] *Laboratório de Ultraestrutura Celular Hertha Meyer, Instituto de Biofísica Carlos Chagas Filho, Centro de Ciências da Saúde, Universidade Federal do Rio de Janeiro, UFRJ, Avenida Carlos Chagas Filho, 343, Bloco G, Subsolo, Cidade Universitária, Ilha do Fundão, Rio de Janeiro, CEP 21941-590, Brasil*
[2] *Instituto Nacional de Ciência e Tecnologia em Biologia Estrutural e Bioimagens, Brasil*
[3] *BAMBOO Team, INRIA Grenoble-Rhône-Alpes, Villeurbanne, France*
[4] *Laboratoire de Biométrie et Biologie Evolutive, Université de Lyon, Université Lyon 1, CNRS, UMR5558, Villeurbanne, France*
[5] *Laboratório Nacional de Computação Científica, Av. Getúlio Vargas, 333, Quitandinha, Petrópolis, RJ, CEP: 25651-075, Brasil*
[6] *Instituto Nacional de Metrologia, Qualidade e Tecnologia – Inmetro, Rio de Janeiro, RJ, Brasil*
[7] *Laboratório Intermediário de Biomembranas, Instituto de Biofísica Carlos Chagas Filho, Centro de Ciências da Saúde, Universidade Federal do Rio de Janeiro, UFRJ, Avenida Carlos Chagas Filho, 343, Bloco C, Cidade Universitária, Ilha do Fundão, Rio de Janeiro, CEP 21941-590, Brasil*
[8] *Laboratório de Bioenergética e Fisiologia Mitocondrial, Programa de Biofísica e Bioquímica Celular, Instituto de Bioquímica Médica, Centro de Ciências da Saúde, Universidade Federal do Rio de Janeiro, UFRJ, Avenida Carlos Chagas Filho, 343, Bloco D SS sala 13, Cidade Universitária, Ilha do Fundão, Rio de Janeiro, CEP 21941-590, Brasil*

SUMMARY

Certain trypanosomatids co-evolve with an endosymbiotic bacterium in a mutualistic relationship that is characterized by intense metabolic exchanges. Symbionts were able to respire for up to 4 h after isolation from *Angomonas deanei*. FCCP (carbonyl cyanide-4-(trifluoromethoxy)phenylhydrazone) similarly increased respiration in wild-type and aposymbiotic protozoa, though a higher maximal O_2 consumption capacity was observed in the symbiont-containing cells. Rotenone, a complex I inhibitor, did not affect *A. deanei* respiration, whereas TTFA (thenoyltrifluoroacetone), a complex II activity inhibitor, completely blocked respiration in both strains. Antimycin A and cyanide, inhibitors of complexes III and IV, respectively, abolished O_2 consumption, but the aposymbiotic protozoa were more sensitive to both compounds. Oligomycin did not affect cell respiration, whereas carboxyatractyloside (CAT), an inhibitor of the ADP-ATP translocator, slightly reduced O_2 consumption. In the *A. deanei* genome, sequences encoding most proteins of the respiratory chain are present. The symbiont genome lost part of the electron transport system (ETS), but complex I, a cytochrome d oxidase, and FoF1-ATP synthase remain. In conclusion, this work suggests that the symbiont influences the mitochondrial respiration of the host protozoan.

Key words: Symbiosis, trypanosomatids, bioenergetics, electron transfer complex, evolution.

INTRODUCTION

The Trypanosomatidae family is well known for comprising protozoa that cause diseases in humans, such as *Trypanosoma cruzi*, the aetiological agent of Chagas disease, *Leishmania* species, which promote different clinical forms of leishmaniasis, and *Trypanosoma brucei gambiense* and *Trypanosoma brucei rhodesiense*, which cause sleeping sickness in sub-Saharan Africa (WHO, 2007). However, most protozoa within this family are not pathogenic to humans and usually inhabit insects throughout the entirety of their life cycle. Such trypanosomatids are named monoxenics, and six species, including *Angomonas deanei*, harbour a symbiotic bacterium within the cytoplasm that has coevolved with the host in a mutualistic relationship. Thus, symbiont-containing trypanosomatids constitute an excellent model to study the origin of organelles and the evolution of the eukaryotic cell (Motta, 2010).

The symbiotic bacteria found in trypanosomatids are classified as Gram-negative prokaryotes of the

* Corresponding authors: M.C.M. Motta: Laboratório de Ultraestrutura Celular Hertha Meyer, Instituto de Biofísica Carlos Chagas Filho, Centro de Ciências da Saúde, Universidade Federal do Rio de Janeiro, UFRJ, Avenida Carlos Chagas Filho, 343, Bloco G, Subsolo, Cidade Universitária, Ilha do Fundão, Rio de Janeiro, CEP 21941-590, Brasil. E-mail: motta@biof.ufrj.br; A. Galina: E-mail: galina@bioqmed.ufrj.br

β-Proteobacteria group and are phylogenetically related to the Alcaligenaceae family (Du *et al*. 1994; Alves *et al*. 2011; Teixeira *et al*. 2011; Motta *et al*. 2013), clustered as a sister group of the *Taylorella* genus (Alves *et al*. 2013*a*, *b*). Previous studies have shown that intensive metabolic interactions occur between the bacterium and the protozoan. The treatment of *A*. *deanei* with chloramphenicol generated an aposymbiotic strain, thereby providing an important tool in the investigation of the bacterium's influence on the host protozoan's metabolism (Mundim *et al*. 1974). Previous research has revealed that symbiont-bearing trypanosomatids present an enhanced growth rate (Frossard *et al*. 2006) and lower nutritional requirements when compared with aposymbiotic strains (Chang *et al*. 1975; Mundim and Roitman, 1977; Fiorini *et al*. 1989). This is related to the fact that the symbiont completes essential metabolic routes of the host trypanosomatid, such as those involving the production of amino acids, vitamins and heme (Alves *et al*. 2011, 2013*a*, *b*; Klein *et al*. 2013). Furthermore, the presence of a symbiotic bacterium promotes alterations in the trypanosomatid ultrastructure (Freymuller and Camargo, 1981), in its surface charge (Oda *et al*. 1984) and in its carbohydrate plasma membrane composition (Esteves *et al*. 1982). In return, the host protozoan protects the symbiont from osmotic lysis because the envelope of the bacterium is composed of two membrane units and a reduced cell wall (Motta *et al*. 1997*a*). Furthermore, some evidence indicates that the endosymbiont exploits the trypanosomatid's energy metabolism by utilizing the ATP generated by host glycosomes (Motta *et al*. 1997*b*).

The mitochondrion is the centre of energy production in eukaryotic cells. Through oxidative phosphorylation, an electron circuit is coupled to ATP production and consumes O_2, the electron's final acceptor. Four complexes that form the electron transport system (ETS) are located in the mitochondrial inner membrane (MIM). Donated by NADH to NADH:ubiquinone oxidoreductase (complex I) or by succinate and $FADH_2$ to succinate:fumarate dehydrogenase (complex II), electrons enter the ETS and promote proton transport from the mitochondrial matrix to the positive site (P side) of the MIM. With the exception of complex II, the other complexes (complex I, cytochrome *bc1*- complex III- and cytochrome *c* oxidase- complex IV [COX]) carry out proton transport and build an electrochemical H^+ gradient. This proton-motive force causes the protons to cross the MIM back into the mitochondrial matrix, which occurs through FoF1-ATP synthase (complex V) while ATP is synthesized from ADP and Pi. In addition to oxidative phosphorylation, the mitochondrion of trypanosomatids receives metabolites from the cytosol and produces precursors for essential biosynthetic pathways. This organelle is considered the main source of reactive oxygen species (ROS) as a by-product of respiration (Guénebaut *et al*. 1998; Grigorieff, 1999; Schägger, 2001; Brandt, 2006; Belevich and Verkhovsky, 2008; Strauss *et al*. 2008; Lenaz and Genova, 2009).

Compounds that specifically inhibit the activity of each complex of the ETS have been used as important tools for evaluating the extent of mitochondrial metabolism in eukaryotic cells (Lenaz and Genova, 2009). Complex I can be inhibited by rotenone, but a rotenone non-sensitive NADH: ubiquinone dehydrogenase has been described in some species, including *T*. *brucei* (Opperdoes and Michels, 2008). Cyanide is a potent inhibitor of complex IV but cannot completely block oxygen consumption in some organisms. In this case, an alternative oxidase (AOX) to COX is responsible for the generation of H_2O molecules from O_2 but has no capacity to pump protons in the ETS (Kronick and Hill, 1974; Edwards and Chance, 1982).

In the present work, we investigated the influence of the symbiotic bacterium on host O_2 consumption by comparing the respiratory chain functioning of wild-type (Wt) and aposymbiotic strains of *A*. *deanei*. Moreover, we identified the respiratory chain genes of this protozoan and its endosymbiont and compared these sequences with available ones from other trypanosomatids and from β-Proteobacteria, which are considered the symbiont's ancestors.

MATERIALS AND METHODS

Cell growth

Wild-type (Wt) and aposymbiotic strains of *A*. *deanei* were grown for 24 h at 28 °C in Warren's culture medium (Warren, 1960) supplemented with 10% foetal calf serum.

Endosymbiont fractions

Cells were grown to log phase for 24 h in 800 mL of Warren's medium. The endosymbiont fraction was obtained using the procedure described by Azevedo-Martins *et al*. (2007).

Oxygen uptake measurements

Oxygen consumption rates were measured using high-resolution respirometry (OROBOROS Oxygraph-O2K). The electrode was calibrated between 0 and 100% saturation with atmospheric oxygen at 28 °C. Oxygen consumption was measured using 10^7 cells mL^{-1} incubated with 2 mL of Krebs–Ringer Buffer Solution containing 119 mM NaCl, 2·5 mM KC1, 1 mM NaH_2PO_4, 2·5 mM $CaCl_2(2H_2O)$, 1·3 mM $MgCl_2(6H_2O)$, 20 mM HEPES and 11 mM D-glucose. In the case of isolated symbionts, the fraction was incubated in a Krebs–Ringer Buffer

solution containing a higher D-glucose concentration (0·2 M) to avoid bacterial lysis.

Different inhibitors were used to evaluate the activity of the mitochondrial respiratory chain: 1·0–12·0 μM rotenone for complex I; 1·0–6·5 mM thenoyltrifluoroacetone (TTFA) for complex II; 0·25–5·50 μM antimycin A for complex III; 4·5–80·0 μM potassium cyanide (KCN) for complex IV; 0·25–8·0 μg mL^{-1} oligomycin and 10·0–300·0 μM carboxyatractyloside (CAT) for FoF1-ATP synthase. Oligomycin binds the Fo portion of complex V, whereas CAT inhibits the ATP-ADP translocator of the same complex. P-trifluoromethoxy carbonyl cyanide phenylhydrazone (FCCP) was used at concentrations of 0·5–10·0 μM to obtain cells with fully uncoupled mitochondrial respiration. Each compound was added to the Krebs–Ringer Buffer solution after the addition of 10^7 cells mL^{-1}. The points on the plots show the mean values and standard deviation (± SD). The number of experimental replications (n) is indicated in the figure captions.

All compounds used in this work were obtained from Sigma-Aldrich (USA).

Statistical analyses

The results were expressed as the mean ± standard error (± SE), and the statistical analyses involved the use of a two-way ANOVA for comparisons between the wild-type and aposymbiotic strains, followed by a *post-hoc* Tukey's test for comparisons between compounds concentrations. Data were considered statistically significant when $P<0·05$. All experiments with compounds utilized a concentration of 10^7 cells mL^{-1}. In the statistical analyses, the cell concentration was normalized to 10^6 cells mL^{-1}, as presented in the results.

Genomic analysis

For the genomic analysis, data for *A. deanei* and its respective symbiotic bacteria were obtained from our previous publication in which DNA extraction and sequencing followed by gene calling and functional annotation were described (Motta *et al*. 2013). All open reading frames (ORFs) identified were deposited at NCBI GenBank within the accession number ID ATMG00000000. Therefore, in this work, the relevant sequences are indicated according to the respective identification number. The reference sequences used in the present genomic analyses were selected from phylogenetically related organisms, as follows: *Leishmania major, Leishmania infantum, T. cruzi* and *Trypanosoma brucei* from TryTripDB, release 3·3, (Aslett *et al*. 2010); *Crithidia fasciculata* from GenBank (Speijer *et al*. 1996); *Escherichia coli, Bordetella parapertussis* and *Allochromatium vinosum* from METACYC (release 15·1 – http://metacyc.org/).

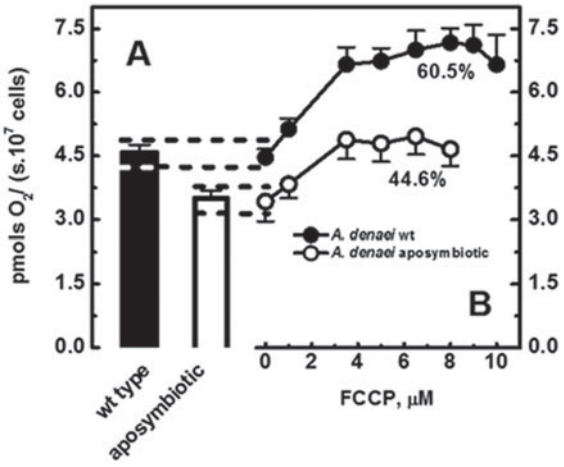

Fig. 1. High-resolution respirometry of *A. deanei* and the uncoupling effect. In (A), the Wt strain (black bar) demonstrates a high oxygen-consumption rate compared with the aposymbiotic strain (white bar) ($n = 7$). In (B), the titration of FCCP increased oxygen consumption in both cells, though the stimulation was different. Wt cells (closed circle) showed increased oxygen consumption by 60·5%, whereas that in aposymbiotic cells (open circles) was increased by 44·6% ($n =$, $P<0·0001$).

RESULTS

Oxygen consumption analyses of A. deanei *strains and isolated symbionts using inhibitors for ETS complexes*

A comparison of the oxygen consumption rates between the wild-type (Wt) and aposymbiotic cells of *A. deanei* revealed that the symbiont-containing protozoan consumes 29·4% more ($P<0·0001$) O_2 than the aposymbiotic strain (Fig. 1A). The Wt cells (10^6 cells) consumed 4·4 pmol O_2* s^{-1} (±0·20), whereas the aposymbiotic strain (also 10^6 cells) consumed 3·4 pmol O_2* s^{-1} (±0·47).

To characterize the functioning of the *A. deanei* respiratory chain, we analysed the effects of classical inhibitors such as oligomycin, rotenone, TTFA, antimycin A and KCN (each one specifically targets a protein complex of ETS) and a respiration uncoupler (FCCP) on the oxygen consumption of non-permeabilized protozoan cells.

FCCP titration was used to reach the maximal respiration rate, which represents full ETS capacity. Both strains reached the maximal respiration rate in the range of 9–15 μM. The data showed that the aposymbiotic strain reached 4·9 pmol O_2* s^{-1}(±0·47) (Fig. 1B), whereas the wild-type cells reached 7·1 pmol O_2* s^{-1}(±0·34) (Fig. 1B). Despite the augmented values, the aposymbiotic strain was less stimulated by FCCP ($P<0·0001$), presenting an increase in oxygen consumption of 44·1%, whereas an enhancement of 61·4% was observed in Wt (Fig. 1B).

Protozoa of both strains were not affected by the complex I inhibitor rotenone up to 45 μM. The small inhibitions observed in Fig. 2A and B ($P<0·0001$) are due to the ethanol that was used as a solvent in the

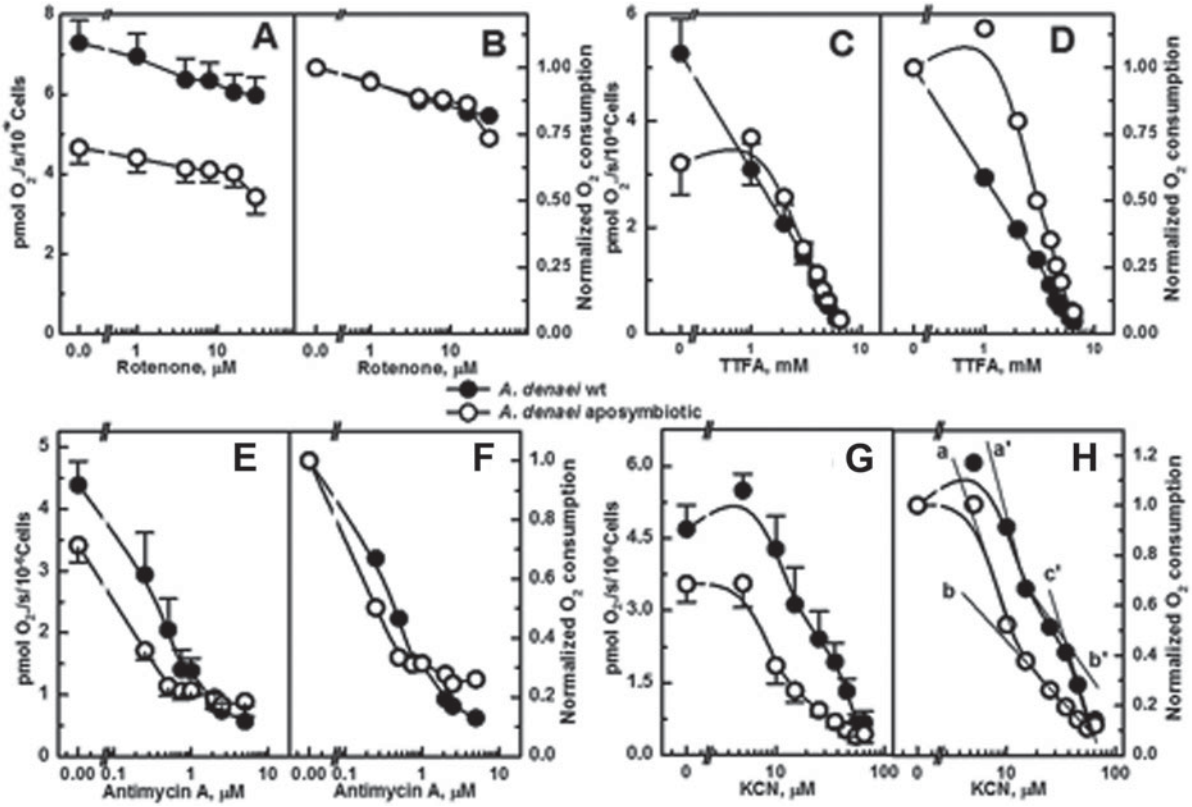

Fig. 2. High-resolution respirometry of Wt and aposymbiotic strains of *A. deanei*. The titration of rotenone is represented in (A) and normalized values of oxygen consumption (0–1) in (B) ($n = 6$). Rotenone did not affect oxygen consumption in either strain; the slight inhibition is due to the ethanol in the stock solution. The titration of TTFA (C) and normalized values of oxygen consumption (0–1) in (D) reveal strongly inhibited oxygen consumption in both strains; the aposymbiotic strain (open circles) was more resistant at a low concentration (1 mM), whereas Wt (closed circles) respiration was reduced by half ($n = 3$, $P < 0{\cdot}0001$). The titration of antimycin A inhibited oxygen consumption of both strains (E); normalized values of oxygen consumption (0–1) are shown in (F). The aposymbiotic strain (open circles) was more sensitive to the inhibitor but became resistant at the concentration of 0·8 μM; the Wt strain (closed circles) was more resistant but was ultimately more strongly inhibited, with a decrease in oxygen consumption by approximately 90% ($n = 5$, $P < 0{\cdot}0101$). Similarly, KCN strongly inhibited both strains (G); normalized values of oxygen consumption (0–1) are shown in (H). For KCN titration, we observed varying slopes (illustrative lines) in both strains due to differing affinity for KCN between the strains. The aposymbiotic strain (open circles) presented two slopes (a and b) on the titration curve; in contrast, the Wt strain (closed circles) presented three slopes (a', b', and c') on the titration curve. The second slope in the Wt strain, b', may be explained by the presence of the symbiotic bacterium increasing the resistance of the host to inhibition by KCN ($n = 5$, $P < 0{\cdot}0001$).

preparation of the rotenone stock solution (data not shown).

To evaluate the contribution of complex II to protozoan respiration, cells were titrated with TTFA, an inhibitor of succinate dehydrogenase activity (Fig. 2C). Our results revealed that the aposymbiotic strain was more resistant to TTFA ($P < 0{\cdot}0001$), with an inhibition of approximately 20% that was detectable only when the cells were exposed to concentrations above 1 mM (Fig. 2D, open circles). In contrast, the symbiont-containing strain was less resistant and was almost 50% inhibited when exposed to 1 mM TTFA (Fig. 2D, closed circles). Both strains were completely inhibited with 6·5 mM TTFA treatment.

The titration curve of antimycin A, an inhibitor of complex III, revealed different sensitivities of the *A. deanei* strains ($P < 0{\cdot}0101$). At a low concentration range (up to 0·4 μM), the aposymbiotic strain showed a greater sensitivity to antimycin A (almost 70% inhibition) compared with that of the symbiont-bearing cells (50% of inhibition) (Fig. 2E–F). However, at concentrations above 0·6 μM, the aposymbiotic strain exhibited respiration that was resistant to antimycin A (70–75%), whereas the Wt strain was almost completely inhibited (90%).

The participation of COX activity in trypanosomatid respiration was investigated using KCN. The data showed that the concentration required to inhibit 50% of respiration was different for the two strains ($P < 0{\cdot}0001$). In the aposymbiotic cells, approximately 8–10 μM KCN provided 50% inhibition, whereas for the symbiont-containing strain, this same value of inhibition was observed with approximately 25–35 μM KCN (Fig. 2G–H). Moreover, the general profile of the KCN inhibition between the two strains was different, suggesting an influence of the

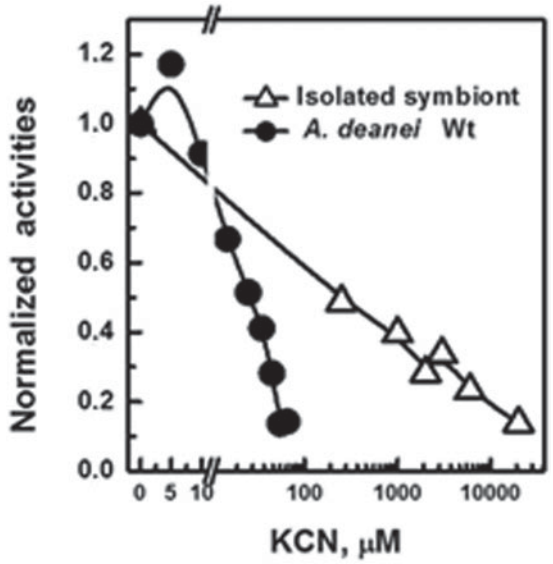

Fig. 3. High-resolution respirometry of *A. deanei*, the symbiont fraction and KCN inhibition. Symbiotic bacteria from the host protozoan can be obtained by cell fractionation. Titration with KCN strongly inhibited oxygen consumption by the symbionts. The graphic is normalized by mg/protein of the symbiotic fraction and shows the Wt strain as closed circles (as Fig. 3D) and the symbiotic fraction as opened triangles. Oxygen consumption by the symbiotic fraction is inhibited by 50% at concentrations of approximately 0·1 mM but is only fully inhibited at concentrations of 20 mM.

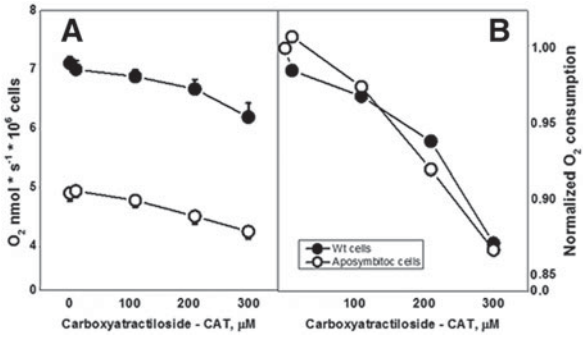

Fig. 4. High-resolution respirometry of Wt and aposymbiotic strains of *A. deanei*. The titration of CAT is represented in (A) and normalized values of oxygen consumption (0–1) in (B) ($n = 3$, $P < 0{\cdot}0001$). CAT affected oxygen consumption in both strains.

symbiont in the global respiration of *A. deanei*, which can be noted in the shape of the curves. The aposymbiotic strain presented two different trends due to different sites of interaction with KCN (Fig. 2H, open circles), whereas the Wt strain curve shows three different trends due to multisite interaction with KCN (Fig. 2H closed circle). This difference is clear after comparing the distinctive slopes obtained for the wild-type strain and the aposymbiotic cells. These slopes were obtained by drawing a line over the inclination of the curve to emphasize each trend.

We also tested the effects of KCN on the symbiont fraction. The same methodology utilized with the cell experiment was adopted for the isolated bacteria. In this case, we fractionated the host protozoa using a pre-established methodology (Azevedo-Martins *et al*. 2007) and incubated the symbionts in Krebs–Ringer buffer solution with 0·2 M D-glucose. The strongest inhibition of symbiont respiration was observed with 20 mM KCN (Fig. 3).

Surprisingly, oligomycin, which inhibits FoF1-ATP synthase, did not reduce oxygen consumption in either strain ($P < 0{\cdot}264$), even at 5 μg mL^{-1}. In the oligomycin incubation experiments, the Wt cells, which presented 5·4 pmol O_2* s^{-1} (±0·3) before the addition of the compound, still consumed the same rate (5·4 pmol O_2* s^{-1}, ±0·2). The aposymbiotic cells presented the same behaviour: 3·4 pmol O_2* s^{-1} before oligomycin (±0·4) and 5·4 pmol O_2* s^{-1} (±0·4) after incubation with oligomycin. However, the use of 300 μM CAT, an ADP-ATP translocator inhibitor, reduced the oxygen consumption of both cells by 13% ($P < 0{\cdot}0001$) (Fig. 4).

Analyses by transmission electron microscopy showed that the different inhibitors used in this study did not affect the ultrastructure of *A. deanei* (data not shown).

Genomic analysis of sequences that encode the complex subunits of the respiratory chain

The annotated genome of *A. deanei* and its symbiont were searched for sequences that encode proteins of the respiratory chain. We considered data that have already been described for trypanosomatids, β-Proteobacteria and other organisms. In relation to complex I, most of the sequences that encode NADH: ubiquinone oxidoreductase were found in *A. deanei* as functional and structural subunits. Based on *T. brucei* published data, 33 nucleus-encoded subunits were identified in this symbiont-bearing species, and one sequence has an orthologue in plant cells (Acestor *et al*. 2011). Another four subunit sequences were identified in the mitochondrion of *A. deanei* (data not shown). All NADH: ubiquinone oxidoreductase subunits were found in the endosymbiont (Table 1).

Almost all of the subunits of succinate: fumarate dehydrogenase (SDH) described in *T. cruzi* were identified in *A. deanei*; however, the genome lacks SDH1, SDH5 and SDH2n (Morales *et al*. 2009) (Table 2). With the exception of SDH4 and SDH9, which are present as a single copy, at least two copies of all other subunits are seemingly present. Similarly, only two subunits that compose cytochrome *bc* oxidase were not present in *A. deanei*: alfa-MMP and beta-MMP (Table 3). Neither complex was found in the genome of the symbiont when gram-negative bacteria (*E. coli* and *Acidithiobacillus ferrooxidans*) were used as reference microorganisms.

Table 1. Complex I subunits of A. deanei and its symbiont. Sequences from Tritrypdb.org and NCBI databases are mentioned in the third column. *T. brucei* and *Escherichia coli* were used as reference organisms to the host trypanosomatid and symbiont analysis, respectively

Subunit	Function	Entry name	Organism	*A. deanei*
NDUFA9/39-kDa	NAD binding site	Tb927.10.13620	*T. brucei*	AGDE_06834; AGDE_12291
NDUFS1/75-kDa	Ferredoxin, 2Fe-2S and 4Fe-4S centre	Tb927.10.12540	*T. brucei*	AGDE_04027
NDUFA6/B14	LYR family	Tb927.10.14860	*T. brucei*	AGDE_01861
NDUFA13/B16.6	NADH regeneration	Tb11.01.0640	*T. brucei*	AGDE_09179; AGDE_02772; AGDE_01567
NDUFB9/B22	LYR family	Tb11.01.7460	*T. brucei*	AGDE_09545; AGDE_03717; AGDE_05311
NDUFA2/B8	NI8M subunit	Tb11.01.8630	*T. brucei*	AGDE_02984; AGDE_01364
NDUFS7/PSST	Quinone binding site	Tb11.47.0017	*T. brucei*	AGDE_09778; AGDE_00485
NDUFAB1/SDAP	ACP co-factor binding site	Tb927.3.860	*T. brucei*	AGDE_03968; AGDE_01170; AGDE_00343
NDUFV1/51-kDa	4Fe-4S centre	Tb927.5.450	*T. brucei*	AGDE_11034
NDUFV2/24-kDa	NAD binding site	Tb927.7.6350	*T. brucei*	AGDE_07927
NDUFA5/B13	–	Tb10.70.3150	*T. brucei*	AGDE_10317; AGDE_03806
Alpha/beta-Hydrolases	Alpha/beta-Hydrolases	Tb09.160.0760	*T. brucei*	AGDE_06832; AGDE_07940; AGDE_04046
Trans-2-enoyl-CoA reductase	NAD(P) binding Rossman domain, alcohool dehydrogenase	Tb09.160.5260	*T. brucei*	AGDE_04330
Trans-2-enoyl-CoA reductase	NAD(P) binding Rossman domain, alcohool dehydrogenase	Tb927.7.7410	*T. brucei*	AGDE_01966; AGDE_01978
DnaJ homologue	DnaJ, Zinc finger	Tb09.211.0330	*T. brucei*	AGDE_09424
NADB_Rossman super family, NDUFA9_like_SDR_a	NAD(P) binding Rossman motif	Tb09.244.2620	*T. brucei*	AGDE_00892
Acyl-CoA synthetase	Acyl-CoA synthetase	Tb927.6.2010	*T. brucei*	AGDE_04709; AGDE_02223; AGDE_09281
Acyl-CoA synthetase	Acyl-CoA synthetase, AMP binding site	Tb11.02.2070	*T. brucei*	AGDE_01480; AGDE_11774
Superoxide dismutase	Fe, Mn superoxide dismutase	Tb11.01.7480	*T. brucei*	AGDE_08825; AGDE_10941; AGDE_05018; AGDE_05571; AGDE_06246
	FMN binding division	Tb927.7.7330	*T. brucei*	AGDE_06154; AGDE_05267; AGDE_08687
LYR motif	LYR motif	Tb11.01.7090	*T. brucei*	AGDE_07329; AGDE_03568; AGDE_02095
Peptidyl-prolyl cis-trans isomerase	Cyclofiline	Tb927.2.1680	*T. brucei*	AGDE_03363
Tetratricopeptide repeat	Tetratricopeptide repeat	Tb927.8.4250	*T. brucei*	AGDE_00201
	NIDM subunit	Tb11.01.1690	*T. brucei*	AGDE_04896; AGDE_04556; AGDE_01601
30 kDa	–	Tb11.02.5070	*T. brucei*	AGDE_11422; AGDE_06025; AGDE_02395; AGDE_04570

Subunit	Function	Entry name	Organism	Symbiont
NuoA	NADH-quinone oxidoreductase subunit A	b2288	*E. coli*	CKCE_0114
NuoB	NADH-quinone oxidoreductase subunit B	b2287	*E. coli*	CKCE_0115
NuoC	NADH-quinone oxidoreductase subunit C	b2286	*E. coli*	CKCE_0116
NuoD	NADH-quinone oxidoreductase subunit D	b2286	*E. coli*	CKCE_0117
NuoE	NADH-quinone oxidoreductase subunit E	b2285	*E. coli*	CKCE_0118
NuoF	NADH-quinone oxidoreductase subunit F	b2284	*E. coli*	CKCE_0119
NuoG	NADH-quinone oxidoreductase subunit G	b2283	*E. coli*	CKCE_0120
NuoH	NADH-quinone oxidoreductase subunit H	b2282	*E. coli*	CKCE_0121
NuoI	NADH-quinone oxidoreductase subunit I	b2281	*E. coli*	CKCE_0122
NuoJ	NADH-quinone oxidoreductase subunit J	b2280	*E. coli*	CKCE_0123
NuoK	NADH-quinone oxidoreductase subunit K	b2279	*E. coli*	CKCE_0124
NuoL	NADH-quinone oxidoreductase subunit L	b2278	*E. coli*	CKCE_0125
NuoM	NADH-quinone oxidoreductase subunit M	b2277	*E. coli*	CKCE_0126
NuoN	NADH-quinone oxidoreductase subunit N	b2276	*E. coli*	CKCE_0127

Table 2. Complex II subunits of *A. deanei*. Sequences from NCBI database are mentioned in the second column. *T. cruzi* was used as reference organism in these analyses. Sequences related to the complex II were not found in the symbiont genome

Subunit	Entry name	Organism	*A. deanei*
SDH2c	XP_803796.1	*T. cruzi* (CL Brener)	AGDE_10548; AGDE_04320
SDH2c	XP_806126.1	*T. cruzi* (CL Brener)	AGDE_10548; AGDE_04320
SDH6a	XP_809065.1	*T. cruzi* (CL Brener)	AGDE_09259; AGDE_03415; AGDE_11796
SDH6a	XP_812789.1	*T. cruzi* (CL Brener)	AGDE_09259; AGDE_03415; AGDE_11796
SDH6b	XP_813603.1	*T. cruzi* (CL Brener)	AGDE_09259; AGDE_03415; AGDE_11796
SDH6b	XP_813645.1	*T. cruzi* (CL Brener)	AGDE_09259; AGDE_03415; AGDE_11796
SDH7	XP_813318.1	*T. cruzi* (CL Brener)	AGDE_09911; AGDE_05191; AGDE_01450
SDH7	XP_820239.1	*T. cruzi* (CL Brener)	AGDE_09911; AGDE_05191; AGDE_01450
SDH3	XP_809410.1	*T. cruzi* (CL Brener)	AGDE_00823; AGDE_00625; AGDE_02254
SDH3	XP_810064.1	*T. cruzi* (CL Brener)	AGDE_00823; AGDE_00625; AGDE_02254
SDH4	XP_808211.1	*T. cruzi* (CL Brener)	AGDE_14671
SDH4	XP_816430.1	*T. cruzi* (CL Brener)	AGDE_14671
SDH8	XP_809192.1	*T. cruzi* (CL Brener)	AGDE_02016; AGDE_01679; AGDE_01996; AGDE_01814
SDH8	XP_817545.1	*T. cruzi* (CL Brener)	AGDE_02016; AGDE_01996; AGDE_0679; AGDE_01814
SDH9	XP_807105.1	*T. cruzi* (CL Brener)	AGDE_02129
SDH10	XP_808894.1	*T. cruzi* (CL Brener)	AGDE_03926; AGDE_00999
SDH10	XP_808903.1	*T. cruzi* (CL Brener)	AGDE_03926; AGDE_00999
SDH11	XP_814088.1	*T. cruzi* (CL Brener)	AGDE_03496; AGDE_00992; AGDE_05781
SDH11	XP_814509.1	*T. cruzi* (CL Brener)	AGDE_03496; AGDE_00992; AGDE_05781

Table 3. Complex III subunits of *A. deanei*. Sequences from Tritrypdb.org and NCBI databases are mentioned in the second column. *T. brucei* was used as reference organism in these analyses. Sequences related to the complex III were not found in the symbiont genome

Subunit	Entry name	Organism	*A. deanei*
Reiske Iron-Sulphur (ISP)	Tb09.211.4700	*T. brucei*	AGDE_01127; AGDE_06632; AGDE_11765; AGDE_11286
Cytochrome c1	Tb927.8.1890	*T. brucei*	AGDE_08215; AGDE_04829
Cytochtome bd ubiquinol oxidase 14 kDa subunit	Tb10.70.2970	*T. brucei*	AGDE_09048; AGDE_01857; AGDE_07658
–	Tb11.01.7900	*T. brucei*	AGDE_09441; AGDE_03239; AGDE_00602; AGDE_05049
Apocytochrome b	AAA32115 (NCBI)	*T. brucei*	AGDE_09441; AGDE_05049; AGDE_03239; AGDE_00602

Many subunits of COX that have been reported for *C. fasciculata* in GenBank (Speijer *et al*. 1996) were also found in *A. deanei* (Table 4). Regarding the *A. deanei* bacterium, a COX from *B. parapertussis* was absent, but a cytochrome d oxidase from the same prokaryote was found in the endosymbiont. Interestingly, the trypanosomatid AOX (Tb10.6k15.3640) that has been identified in *T. brucei* (Tritrypdb.org) was also found in *A. deanei*. The FoF1-ATP synthase subunits were found in the host genome, as well as in the symbiotic bacterium (Table 5). Moreover, the mitochondrial genome (kDNA) presented 10 sequences similar to complexes I (NADH dehydrogenase subunits 1, 2, 4, 5 and 7), III (cytochrome b), IV (subunits I, II and III), and V (ATPase subunit 6) (Table 6). The whole kDNA genome sequence is identified as KJ778684 at NCBI.

DISCUSSION

An intensive metabolic exchange occurs between the host trypanosomatid and its symbiotic bacterium. The symbiont provides essential nutrients and metabolic precursors that complete biosynthetic pathways in the host cell, and the protozoan supplies the symbiont with energy and growth factors (Motta, 2010). For example, the symbiont contains ornithine carbamoyltransferase, which converts ornithine to citrulline, thus completing the urea cycle of the host (Camargo and Freymüller, 1977; Galinari and Camargo, 1978). The urea cycle is involved in amino acid synthesis and also produces intermediate metabolites related to the biosynthesis of pyrimidines, proline and polyamines, which are essential factors in cell growth and differentiation (Herby and Persson, 1990; Alves *et al*. 2013*b*).

The cellular localization of the endosymbiont in *A. deanei* is also evidence of metabolic exchanges. Surrounded by glycosomes, the endosymbiont presents a surface ATPase, which may indicate that ATP provided by the host is hydrolysed, supporting an active transport mechanism in the bacterial envelope (Motta *et al*. 1997*b*). Such a hypothesis was demonstrated in pathogenic intracellular prokaryotes, such as those belonging to the *Rickettsia* and *Chlamydia* genera (Winkler, 1976; Hatch *et al*. 1982).

Table 4. Cytochromes (c and d) and complex IV subunits of *A. deanei* and its symbiont. Sequences from NCBI database are mentioned in the second column. The cytochrome c of *L. major*, the COX subunits of *C. fasciculata* and the AOX of the *T. brucei* (* = Tritrypdb.org) were used as references in the host genome analyses. The symbiont did not present cytochrome c, neither the cytochrome c oxidase. However, sequences codifying a cytochrome d (*A. vinosum*) and cytochrome d oxidase subunits (*B. parapertussis*) were found in the symbiont genome

Subunit	Entry name	Organism	*A. deanei*
Cytochrome c	XP_001682213.1	*L. major* strain Friedlin	AGDE_04892; AGDE_04032; AGDE_01854
Cytochrome c oxidase subunit precursor	AAB05893.1	*C. fasciculata*	AGDE_04026; AGDE_03061; AGDE_00221
Cytochrome c oxidase subunit 10	AAB50892.1	*C. fasciculata*	AGDE_02665; AGDE_02191; AGDE_02080
Cytochrome c oxidase subunit 8	AAB50891.1	*C. fasciculata*	AGDE_04026; AGDE_03061; AGDE_00221
Cytochrome c oxidase subunit 6	AAB50890.1	*C. fasciculata*	AGDE_02976; AGDE_02832; AGDE_02832; AGDE_01766; AGDE_01436; AGDE_00501
Cytochrome c oxidase subunit 9	AAB50889.1	*C. fasciculata*	AGDE_12388; AGDE_04535; AGDE_00903
Cytochrome c oxidase subunit 7	AAB50888.1	*C. fasciculata*	AGDE_04566; AGDE_02181
Cytochrome c oxidase subunit 5	AAB50887.1	*C. fasciculata*	AGDE_04161; AGDE_02818
Cytochrome c oxidase:SUBUNIT = 8	2207221A	*C. fasciculata*	AGDE_04026; AGDE_03061; AGDE_00221
Alternative oxidase	Tb10.6k15.3640*	*T. brucei*	AGDE_08853; AGDE_05278
Subunit	**Entry name**	**Organism**	**Symbiont**
Cytochrome d	ADA70141.1	*A. vinosum*	WP_015238747
Cytochrome D ubiquinol oxidase subunit I	CAE39308.1	*B. parapertussis*	WP_015238748
Cytochrome D ubiquinol oxidase subunit II	CAE39308.1	*B. parapertussis*	WP_015238747

In addition, the symbiont and the host endoplasmic reticulum, where most phospholipid biosynthesis occurs, are closely associated. Inhibitors of phosphatidylcholine biosynthetic pathways affect the symbiont's phospholipid composition (Bernard *et al*. 2006; Palmié-Peixoto *et al*. 2006), and isolated symbionts demonstrate a marked reduction in phosphatidylcholine production, thereby indicating that the bacterium can obtain a portion of this phospholipid from the host cell. In accordance with this idea, the symbiont enhances the glycerophospholipid metabolism of the host protozoan (Azevedo-Martins *et al*. 2007).

Given the accelerated metabolism of the Wt strain and the capacity of isolated symbionts to metabolize, we can suggest that symbiont-containing cells present an increased demand for energy. This point may justify in part the high rate of oxygen consumption of such protozoa in comparison to aposymbiotic cells, as demonstrated experimentally in this work. The increase in oxygen consumption may also be related to an enhanced production of metabolic intermediates by the symbiont. For example, the augmented amino acid production in the host's urea cycle may directly furnish substrates to the Krebs cycle, thereby increasing electron donation to the mitochondrion and its ETS capacity (maximal uncoupled respiration). It is also worth considering that the isolated bacteria are able to respire, thus presenting their own operative and functional ETS. This indicates that the total amount of oxygen consumption in trypanosomatids is increased due to the presence of the symbiont.

The complex I, NADH: ubiquinone oxidoreductase from *A. deanei* is rotenone non-sensitive. Although many subunits of this complex were identified in the *A. deanei* genome, the lack of an effect of this inhibitor has been reported in the literature for other protozoa of the Trypanosomatidae family, such as *T. brucei* (Opperdoes and Michels, 2008). Regarding complex II, many of the 12 subunits identified in *T. brucei* (Morales *et al*. 2009) were also found in the *A. deanei* genome, and the use of TTFA inhibited oxygen consumption in this species. However, this complex appears to be absent in the genome of the endosymbiont. The data presented in Fig. 2 are puzzling. Indeed, the total respiration of the aposymbiotic strain is decreased by the absence of the symbiont, though an increased amount of the TTFA inhibitor is needed to cause 50% inhibition in this strain. This may indicate that a compensatory mechanism for the expression of complex II may be operating and that the presence of the symbiont may suppress this expression. Regardless, it is worth considering that the regulation of ROS production might be directly influencing this complex and that the use of TTFA is known to increase ROS. Further studies are needed to test these hypotheses.

Cytochrome *bc* oxidase (complex III) genes are absent in the symbiont genome but are present in the host trypanosomatid genome. The genomic data are

Table 5. Complex V subunits of *A. deanei* and its symbiont. Sequences from TriTrypDB and NCBI databases are mentioned in the second column. Sequences codifying complex V subunits in *C. fasciculata* and *L. major* were used as reference in host genome searches. *E. coli* was used as a reference in the symbiont genome analyses

Subunit	Entry name	Organism	*A. deanei*
3 (Fo portion)		*C. fasciculata*	AGDE_03804; AGDE_07390; AGDE_05004
5 (Fo portion)		*C. fasciculata*	AGDE_03856; AGDE_02485
6 (Fo portion)		*C. fasciculata*	AGDE_01588; AGDE_01375
epsilon (F1 largest portion)		*C. fasciculata*	AGDE_06810; AGDE_05707
ATPase alpha subunit	LmjF.05.0500	*L. major*	AGDE_09011; AGDE_03271; AGDE_05341; AGDE_05991; AGDE_00066; AGDE_00224; AGDE_10468; AGDE_02849
ATPase subunit 9, putative	LmjF.21.0740, LmjF.26.0460	*L. major*	AGDE_09118; AGDE_05921; AGDE_07804; AGDE_03088
ATP synthase, putative	LmjF.21.1340	*L. major*	AGDE_04698; AGDE_03791
ATP synthase F1 subunit gamma protein, putative	LmjF.21.1770	*L. major*	AGDE_11312; AGDE_00941; AGDE_03076
(H)-ATPase G subunit, putative	LmjF.23.0340	*L. major*	AGDE_04470; AGDE_01787
ATP synthase, epsilon chain, putative	LmjF.30.3600	*L. major*	AGDE_10416; AGDE_03733; AGDE_02388; AGDE_02184
ATP synthase, putative	LmjF.36.3100	*L. major*	AGDE_07202; AGDE_05022; AGDE_04961
Subunit	Entry name	Organism	Symbiont
Fo complex, a subunit	b3738	*E. coli*	CKCE_0657
Fo complex, b subunit	b3736	*E. coli*	CKCE_0659
Fo complex, c subunit	b3737	*E. coli*	CKCE_0658
F1 complex, α subunit	b3734	*E. coli*	CKCE_0661
F1 complex, β subunit	b3732	*E. coli*	CKCE_0663
F1 complex, γ subunit	b3733	*E. coli*	CKCE_0662
F1 complex, δ subunit	b3735	*E. coli*	CKCE_0660
F1 complex, ε subunit	b3731	*E. coli*	CKCE_0664

Table 6. Mitochondrial sequences in kDNA of *A. deanei*. The reference sequences are from TriTrypDB database. The second column indicates the complex of the sequence

Subunit	Complex
NADH dehydrogenase subunit 1	I
NADH dehydrogenase subunit 2	I
NADH dehydrogenase subunit 4	I
NADH dehydrogenase subunit 5	I
NADH dehydrogenase subunit 7	I
Cytochrome b	III
cytochrome c oxidase subunit I	IV
cytochrome c oxidase subunit II	IV
cytochrome c oxidase subunit III	IV
ATPase subunit 6	V

in accordance with the high-resolution respirometry findings for the specific inhibitor of complex III antimycin A, which was able to inhibit oxygen consumption by *A. deanei*. However, the amount of antimycin A needed to cause 50% inhibition in the aposymbiotic strain was lower (up to 0·8 μM) in comparison to the Wt strain. The lack of inhibition observed at higher antimycin A concentrations in the aposymbiotic strain compared with the Wt strain may indicate a compensatory mechanism for the expression of the subunits of complex III. Alternatively, an imbalance in the steady-state levels of ROS caused by the absence of the symbiont could modulate the signalling of redox pathway factors, thereby affecting the expression of other oxidases not sensitive to antimycin A or involved in oxidative phosphorylation. Further studies are needed to clarify these alterations in the bioenergetics in *A. deanei*.

In contrast, not all subunits that compose mitochondrial complex IV were identified in the *A. deanei* genome, but the use of KCN completely abolished the protozoan's oxygen consumption. Interestingly, a trypanosomatid AOX was also found in the *A. deanei* genome, similar to what was previously described for *T. brucei* (Aslett *et al*. 2010). However, the strong inhibition observed in this work with KCN (at concentrations above 100 μM, almost 95% of total respiration was arrested) indicates that this AOX is inactive or not expressed in *A. deanei*. Furthermore, in the high-resolution respirometry of *A. deanei* during KCN titration, the symbiont-containing and symbiont-free cells presented different sensitivities to this inhibitor, thereby indicating a complex interaction between cyanide and COX sites.

This fact may be related to the amount of COX involved in different cellular states of respiration, which may vary in accordance to the energy requirements. In other words, not all COX units are involved in respiration, and the excess units are considered to be spare COX units that are used to reach maximum respiration (Bernard *et al*. 2006). Thus, titration with KCN in the Wt strain may affect these reservoirs of COX, which may show different KCN affinities. However, the aposymbiotic strain did not show all the slopes detected in the Wt strain (as marked by lines a and b in Fig. 2H). A possible explanation could be that the amount and interactions among COX units were decreased by the absence of symbiotic COX units. In fact, in parallel experiments using isolated symbionts, we were able to detect KCN inhibition of respiration with a single component and with a low affinity for KCN (Fig. 3).

Several subunits of complex V, composed by FoF1-ATP synthase, were found in the genomes of *A*. *deanei* and its symbiont. However, oligomycin, a specific inhibitor of this complex, did not affect oxygen consumption by the protozoan. This can be explained by the absence of some Fo subunits in the host that are the target of oligomycin. Conversely, CAT, an ADP-ATP translocator inhibitor, slightly affected the oxygen consumption in both strains. Thus, the data indicate that the *A*. *deanei* mitochondrion presents ETS-dependent oxygen consumption that is uncoupled from ATP production.

CONCLUSIONS/FUTURE DIRECTIONS

In this work, we conclude that the presence of the symbiont enhances the trypanosomatid's oxygen consumption. The symbiont-bearing and the symbiont-free strains of *A*. *deanei* showed differences in their energetic metabolism and distinct sensitivities when treated with inhibitors that specifically affect each mitochondrial complex of the electron transport chain. The symbiont-containing protozoa appear to be more resistant to these compounds than the aposymbiotic cells. This may be related to the fact that essential biosynthetic routes are completed by the bacterium in the symbiont-bearing trypanosomatids, improving the metabolism of the host. It is also worth considering that differences in O_2 consumption may be related to compensatory mutations that may have arisen in the aposymbiotic strain to optimize its respiration in the absence of the symbiont. According to this idea, a single amino acid change in the nucleus-encoded F1 subunit of ATP synthase is able to compensate for energy-demanding activity in dyskinetoplastic cells of *T*. *brucei* that lacks the Fo portion, which is essential for electrochemical potential maintenance (Dean *et al*. 2013).

Another important aspect that should be considered is that the symbiont demands energy molecules from the host cell to maintain optimal physiology. This is most likely related to an enhanced respiration capacity in symbiont-bearing trypanosomatids when compared with aposymbiotic cells and a ROS regulatory activity of the host mitochondria. In accordance with this idea, our genome database searches showed that the symbiont genome lacks important components of the respiratory chain. Further studies are necessary to explain how the absence of complex II in the bacterium can affect the exchange of intermediates between both partners in this symbiotic relationship.

ACKNOWLEDGEMENTS

Special thanks to Dr Ronir Raggio Luiz from Instituto de Estudos em Saúde Coletiva (IESC) for the statistical analyses.

FINANCIAL SUPPORT

This work was supported by Coordenação de Aperfeiçoamento de Pessoal de Nível Superior (CAPES), Fundação Carlos Chagas Filho de Amparo à Pesquisa do Estado do Rio de Janeiro (FAPERJ), Centro Nacional de Desenvolvimento Científico e Tecnológico (CNPq) and Instituto Nacional de Ciência e Tecnologia em Excitotoxicidade e Neuroproteção (INCTEN). This work was also supported by European Research Council under the European Community's Seventh Framework Programme (FP7/2007-2013)/ERC grant agreement no. (247073)10.

REFERENCES

Acestor, N., Zíková, A., Dalley, R. A., Anupama, A., Panigrahi, A. K. and Kenneth, D. S. (2011). *Trypanosoma brucei* mitochondrial respiratome: composition and organization in procyclic form. *Molecular Cell Proteomics* **10**, M110.006908.

Alves, J. M. P., Voegtly, L., Matveyev, A. V., Lara, A. M., Silva, F. M., Serrano, M. G., Buck, G. A., Teixeira, M. M. G. and Camargo, E. P. (2011). Identification and phylogenetic analysis of heme synthesis genes in trypanosomatids and their bacterial endosymbionts. *PLOS ONE* **6**, e23518.

Alves, J. M., Klein, C. C., da Silva, F. M., Costa-Martins, A. G., Serrano, M. G., Buck, G. A., Vasconcelos, A. T., Sagot, M. F., Teixeira, M. M., Motta, M. C. M. and Camargo, E. P. (2013*a*). Endosymbiosis in trypanosomatids: the genomic cooperation between bacterium and host in the synthesis of essential amino acids is heavily influenced by multiple horizontal gene transfers. *BMC Evolutionary Biology* **13**, 190. doi: 10.1186/1471-2148-13-190.

Alves, J. M., Serrano, M. G., Maia da Silva, F., Voegtly, L. J., Matveyev, A. V., Teixeira, M. M., Camargo, E. P. and Buck, G. A. (2013*b*). Genome evolution and phylogenomic analysis of Candidatus Kinetoplastibacterium, the betaproteobacterial endosymbionts of Strigomonas and Angomonas. *PLOS ONE* **5**, 338–350. doi: 10.1093/gbe/evt012.

Aslett, M., Aurrecoechea, C., Berriman, M., Brestelli, J., Brunk, B. P., Carrington, M., Depledge, D. P., Fisher, S., Gajria, B., Gao, X., Gardner, M. J., Gingle, A., Grant, G., Harb, O. S., Heiges, M., Hertz-Fowler, C., Houston, R., Innamorato, F., Iodice, J., Kissinger, J. C., Kraemer, E., Li, W., Logan, F. J., Miller, J. A., Mitra, S., Myler, P. J., Nayak, V., Pennington, C., Phan, I., Pinney, D. F., Ramasamy, G., Rogers, M. B., Roos, D. S., Ross, C., Sivam, D., Smith, D. F., Srinivasamoorthy, G., Stoeckert, C. J., Subramanian, S., Thibodeau, R., Tivey, A., Tratman, C., Velarde, G. and Wang, H. (2010). TriTryDB: a functional genomic resource for the Trypanosomatidae. *Nucleic Acids Research* **38**, D457–D463. doi: 10.1093/nar/gkp851.

Azevedo-Martins, A. C., Frossard, M. L., de Souza, W., Einicker-Lamas, M. and Motta, M. C. M. (2007). Phosphatidylcholine synthesis in

Crithidia deanei: the influence of the endosymbiont. *FEMS Microbiology Letters* **275**, 229–236.

Belevich, I. and Verkhovsky, M. I. (2008). Molecular mechanism of proton translocation by cytochrome c oxidase. *Antioxidants and Redox Signaling* **10**, 1–29.

Bernard, G., Faustin, B., Passerieux, E., Galinier, A., Rocher, C., Bellance, N., Delage, J. -P., Casteilla, L., Letellier, T. and Rossignol, R. (2006). Physiological diversity of mitochondrial oxidative phosphorylation. *American Journal of Physiology Cell Physiology* **291**, C1172–C1182.

Brandt, U. (2006). Energy converting NADH:quinone oxidoreductase (complex I). *Annual Review in Biochemistry* **75**, 69–92.

Camargo, E. P. and Freymüller, E. (1977). Endosymbiont as supplier of ornithine carbamoyltransferase in a trypanosomatid. *Nature* **270**, 52–53.

Chang, K. P., Chang, C. S. and Sassa, S. (1975). Heme biosynthesis in bacterium-protozoon symbioses: enzymic defects in host hemofagellates and complemental role of their intracellular symbiotes. *Proceedings of the National Academy of Sciences USA* **72**, 2979–2983.

Dean, S., Gould, M. K., Dewar, C. E. and Schnaufer, A. C. (2013). Single point mutations in ATP synthase compensate for mitochondrial loss in trypanosomatids. *Proceedings of the National Academy of Sciences USA* **110**, 14741–14746.

Du, Y., McLaughlin, G. and Chang, K. P. (1994). 16S ribosomal DNA sequence identies of β- proteobacterial endosymbionts in three *Crithidia* species. *Journal of Bacteriology* **176**, 3081–3084.

Edwards, C. and Chance, C. (1982). Evidence for the presence of two terminal oxidases in the trypanosomatid *Crithidia oncopelti*. *Journal of General Microbiology* **128**, 1409–1414.

Esteves, M. J. G., Andrade, A. F. B., Angluster, J., de Souza, W., Mundim, M. H., Roitman, I. and Pereira, M. E. A. (1982). Cell surface carbohydrates in *Crithidia deanei*: influence of the endosymbiont. *European Journal of Cell Biology* **28**, 244–248.

Fiorini, J. E., Faria e Silva, P. M., Soares, M. J. and Brasil, R. P. (1989). Três novas espécies de tripanosomatídeos de insetos isolados em Alfenas, Minas Gerais, Brasil. *Memórias do Instituto Oswaldo Cruz* **84**, 69–74.

Freymuller, J. E. and Camargo, E. P. (1981). Ultrastructural differences between species of trypanosomatids with and without endosymbionts. *Journal of Protozoology* **28**, 175–182.

Frossard, M. L., Seabra, S. H., DaMatta, R. A., de Souza, W., de Mello, F. G. and Motta, M. C. M. (2006). An endosymbiont positively modulates ornithine decarboxylase in host trypanosomatids. *Biochemical and Biophysical Research Communications* **343**, 443–449.

Galinari, S. and Camargo, E. P. (1978). Trypanosomatid protozoa: survey of acetylornithinase and ornithine acetyltransferase. *Experimental Parasitology* **46**, 277–282.

Grigorieff, N. (1999). Structure of the NADH:quinone oxidoreductase (complex I). *Current Opinion in Structural Biology* **9**, 476–483.

Guénebaut, V., Schlitt, A., Weiss, H., Leonard, K. and Friedrich, T. (1998). Consistent structure between bacterial and mitochondrial NADH: quinone oxidoreductase (complex I). *Journal of Molecular Biology* **276**, 105–112.

Hatch, T. P., Al-Hossainy, E. and Silverman, J. A. (1982). Adenine nucleoside and lysine transport in *Chlamydia psittaci*. *Journal of Bacteriology* **150**, 662–670.

Herby, O. and Persson, L. (1990). Molecular genetics of polyamine synthesis in eukaryotic cells. *Trends Biochemistry Sciences* **15**, 153–158.

Klein, C. C., Alves, J. M., Serrano, M. G., Buck, G. A., Vasconcelos, A. T., Sagot, M. F., Teixeira, M. M., Camargo, E. P. and Motta, M. C. M. (2013). Biosynthesis of vitamins and cofactors in bacterium-harbouring trypanosomatids depends on the symbiotic association as revealed by genomic analyses. *PLOS ONE* **8**, e79786. doi: 10.1371/journal.pone.0079786.

Kronick, P. and Hill, G. C. (1974). Evidence for the functioning of cytochrome o in kinetoplastida. *Biochimica Biophysica Acta* **368**, 173–180.

Lenaz, G. and Genova, M. L. (2009). Structural and functional organization of the mitochondrial respiratory chain: a dynamic super-assembly. *International Journal of Biochemistry and Cell Biology* **41**, 1750–1772.

Morales, J., Mogi, T., Mineki, S., Takashima, E., Mineki, R., Hirawake, H., Sakamoto, K., Ōmura, S. and Kita, K. (2009). Novel mitochondrial Complex II isolated from *Trypanosoma cruzi* is composed of 12 peptides including a heterodimeric Ip subunit. *Journal of Biological Chemistry* **284**, 7255–7263.

Motta, M. C. M. (2010). Endosymbiosis in trypanosomatids as a model to study cell evolution. *Open Parasitology Journal* **4**, 139–147.

Motta, M. C. M., Monteiro-Leal, L. H., de Souza, W., Almeida, D. F. and Ferreira, L. C. S. (1997*a*). Detection of penicilin-binding proteins in endosymbiosis of the trypanosomatid *Crithidia deanei*. *Journal of Eukaryotic Microbiology* **44**, 492–496.

Motta, M. C. M., Soares, M. J., Attias, M., Morgado, J., Lemos, A. P., Saad-Nehme, J., Meyer-Fernandes, J. R. and De Souza, W. (1997*b*). Ultrastructural and biochemical analysis of the relationship of *Crithidia deanei* with its endosymbiont. *European Journal of Cellular Biology* **72**, 370–377.

Motta, M. C., Martins, A. C., de Souza, S. S., Catta-Preta, C. M., Silva, R., Klein, C. C., de Almeida, L. G., de Lima Cunha, O., Ciapina, L. P., Brocchi, M., Colabardini, A. C., de Araujo Lima, B., Machado, C. R., de Almeida Soares, C. M., Probst, C. M., de Menezes, C. B., Thompson, C. E., Bartholomeu, D. C., Gradia, D. F., Pavoni, D. P., Grisard, E. C., Fantinatti-Garboggini, F., Marchini, F. K., Rodrigues-Luiz, G. F., Wagner, G., Goldman, G. H., Fietto, J. L., Elias, M. C., Goldman, M. H., Sagot, M. F., Pereira, M., Stoco, P. H., de Mendonça-Neto, R. P., Teixeira, S. M., Maciel, T. E., de Oliveira Mendes, T. A., Ürményi, T. P., de Souza, W., Schenkman, S. and de Vasconcelos, A. T. (2013). Predicting the proteins of *Angomonas deanei, Strigomonas culicis* and their respective endosymbionts reveals new aspects of the trypanosomatidae family. *PLOS ONE* **8**, e60209. doi: 10.1371/journal.pone.0060209.

Mundim, M. H. and Roitman, I. (1977). Extra nutritional requirements of artificially aposymbiotic *Crithidia deanei*. *Journal of Protozoology* **24**, 329–331.

Mundim, M. H., Roitman, I., Hermans, M. A. and Kitajima, E. W. (1974). Simple nutrition of *Crithidia deanei*, a reduviid trypanosomatid with an endosymbiont. *Journal of Protozoology* **21**, 518–521.

Oda, L. M., Alviano, C. S., Costa e Silva Filho, F., Angluster, J., Roitman, I. and De Souza, W. (1984). Surface anionic group in symbiont-bearing and symbiont-free strains of *Crithidia deanei*. *Journal of Protozoology* **31**, 131–134.

Opperdoes, F. R. and Michels, P. A. (2008). Complex I of trypanosomatids: does it exist? *Trends in Parasitology* **24**, 310–317.

Palmié-Peixoto, I., Rocha, M. R., Urbina, J., De Souza, W., Einicker-Lamas, M. and Motta, M. C. M. (2006). Effects of sterol-biosynthesis inhibitors on endosymbiont-bearing trypanosomatids. *FEMS Microbiology Letters* **255**, 33–42.

Schägger, H. (2001). Respiratory supercomplexes. *IUBMB Life* **52**, 119–128.

Speijer, D., Breek, C. K. D., Muijsers, A. O., Groenevelt, P. X., Dekker, H., De Haan, A. and Benne, R. (1996). The sequence of a small subunit of cytochrome c oxidase from *Crithidia fasciculata* which is homologous to mammalian subunit IV. *FEBS Letters* **381**, 123–126.

Strauss, M., Hofhaus, G., Schöder, R. R. and Kühlbrandt, W. (2008). Dimer ribbons of ATP synthase shape the inner mitochondrial membrane. *EMBO Journal* **27**, 1154–1160.

Teixeira, M. M. G., Borghesan, T. C., Ferreira, R. C., Santos, M. A., Takata, C. S. A., Campaner, M., Nunes, V. L. B., Wilder, R. V., De Souza, W. and Camargo, E. P. (2011). Phylogenetic validation of the genera *Angomonas* and *Strigomonas* of trypanosomatids harboring bacterial endosymbionts with the description of new species of trypanosomatids and of proteobacterial symbionts. *Protist* **162**, 503–524.

Warren, L. G. (1960). Metabolism of *Schizotrypanum cruzi*, Chagas. I. Effect of culture age and substrate concentration on respiratory rate. *Journal of Parasitology* **46**, 529–539.

Winkler, H. H. (1976). Rickettsial permeability. An ADP-ATP transport system. *Journal of Biological Chemistry* **251**, 389–396.

World Health Organization (2007). Update of American trypanosomiasis and leishmania control and research: final report. Pan American Health Organization/World Health Organization, Rio de Janeiro.